New UWB BPF with Steep Selectivity Based on T-Resonator and Capacitively Coupled $\lambda/4$ and $\lambda/2$ Line Sections

Thai Hoa Duong[1] · Ihn Seok Kim[2]

Abstract

In this paper, two new circuit structures for European and U.S. ultra-wide band(UWB) bandpass filters(BPFs) with sharp roll-off characteristics are introduced. We show first that the ultra-wide bandpass property is obtained from a $\lambda/4$ open T resonator with a capacitively coupled $\lambda/4$ short-circuited line, which provides two attenuation poles at lower and upper cutoff frequencies. Then, two identical capacitively coupled input/output lines, which can be $\lambda/4$-length open ends or $\lambda/2$-length short ends, with the T-resonator, are adopted to suppress lower and higher frequency components outside of the pass band. There is coupling between the input and output lines providing two additional transmission zeros in the lower and upper transition bands of the filter. Since the coupling between the T-resonator with the $\lambda/4$ short-circuited line and the input/output lines limits the bandwidth of the filter to the European UWB band, both the $\lambda/4$ short-circuited line and the input/output lines are inserted between the two stacked T-resonators for the U.S. UWB band. The filter structures are simulated with ADS and HFSS and realized with low-temperature co-fired ceramic(LTCC) green tape which has the dielectric constant of 7.8. Measurement results agree well with HFSS simulation results.

Key words : Ultra-Wide Band, BPF, Odd Mode Resonator, T-Resonator, Capacitively Coupled.

I. Introduction

Ultra-wide band(UWB) technology has been making great progress in the development of new high-speed indoor and hand-held wireless communication systems since the unlicensed use of UWB was approved worldwide. As one of the essential components in UWB communication systems, the UWB bandpass filter(BPF) with such characteristics as compact size, good selectivity and stopband rejection, low insertion loss, and low cost has been required. Especially, in order to meet UWB radiation limits, steep selectivity at lower and upper ends of pass band is a characteristic UWB systems must possess[1].

After Saito first introduced a UWB BPF, a number of reports on UWB BPF research and development have been published[2]~[14]. In these reports, filters in [8] and [12]~[14] show the characteristics of steep skirt selectivity and compact size. The filter characteristics, in terms of pass band, circuit structure, technology, insertion loss, return loss, group delay, roll-off slope at lower transition band, number of transmission zeros, and size are compared in Table 1, which also shows a comparison with the results of our own study using single and double T-resonators.

T-resonators, which show odd mode resonant characteristics, have been used in many microwave applications[15]~[23]. In [15]~[17], the T-resonator was originally used to characterize wide band electrical properties of substrate materials at microwave frequencies. In [18] and [19], the T-resonators were designed for RF Micro-

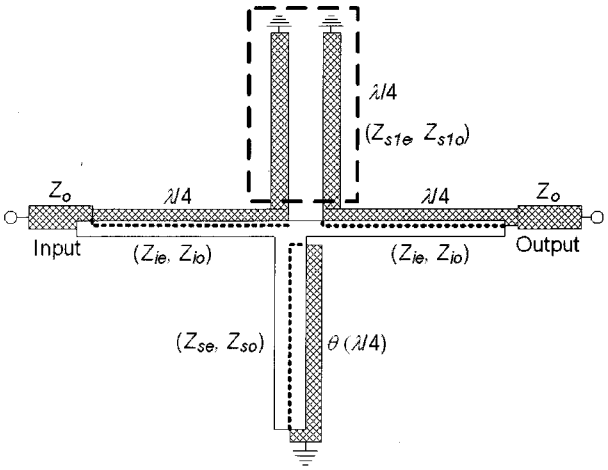

Fig. 1. Schematic for the proposed filter. $\lambda/4$ open T-resonator(empty section), capacitively coupled $\lambda/4$ short-circuited line(lower shaded section), and capacitively coupled two types of input/output lines($\lambda/4$-length open line or $\lambda/2$-length short line sections in the upper shaded section).

Manuscript received May 29, 2009 ; revised August 7, 2009. (ID No. 20090529-03J)
College of Electronics & Information, Kyunghee University, Yongin, Korea.

Table 1. Comparison of characteristics of various UWB BPFs with steep skirt selectivity.

Parameters	[8]	[12]	[13]	[14]	This work	
					Single T-resonator	Double T-resonator
Pass band(GHz)	3.5~10.6	3.1~10.6	3.2~4.8	3.1~10.6	3.4~8.5	3.1~10.6
Circuit structure	Composite microstrip/coplanar waveguide	Edge-coupled microstrip/stepped impedance open stub	Left-handed property's interdigital coupled line	5 $\lambda_0/4$ SIR/short stub	Capacitively coupled T resonator	
Technology	PCB	PCB	PCB	PCB	LTCC	
Insertion loss(dB)	0.48	0.5	1.0	0.65	0.9	0.8
Return loss(dB)	17.2	18	13	18	14	17
Group delay(ns)	0.5	0.21	0.49	0.5	0.26	0.22
Roll-off slope at lower transition band(dB/GHz)	64	50	46	65	96	67
Number of transmission zeros	2	2	2	2	4	4
Size(mm^2)	8×11.9	18.6×13.5	20×20	10×18.82	10×10	9×9

Electro-Mechanical(MEM) switch applications. In [20]~[23], BPFs were also developed by using various forms of the T-resonators for narrow and wide band microwave systems based on edge coupling.

All of the above filter applications using various forms of the T-resonators have been based on side-coupling on the same substrate plane. This paper adopts the broadside coupling structure of the T-resonator. Two UWB BPFs are introduced based on a capacitively coupled $\lambda/4$ open T-resonator with the $\lambda/4$ short-circuited line and with input/output lines for the European and the U.S UWB bands. In Section Ⅱ, we first introduce a design theory for the T-resonator based UWB BPF. The design theory explains how to obtain two transmission zeros based on a capacitively coupled $\lambda/4$ short-circuited line, how to add the input and output lines to provide two additional transmission zeros at lower and upper stopbands. The equivalent network and ADS simulation are also included in the section. However, the filter technology cannot be applied for the U.S. UWB band due to bandwidth limitation of the structure involved. To overcome the limitation, both the $\lambda/4$ short-circuited line and the input/output lines were inserted between two identical stacked T-resonators to the U.S. UWB band in this study. HFSS simulation and measurement results for the filters are given in Section Ⅲ.

Ⅱ. Design Theory

2-1 Capacitively Coupled Single $\lambda/4$ Open T Resonator

A UWB BPF for the European band has a circuit structure as shown in Fig. 1. The filter consists of a $\lambda/4$ open T-resonator with a capacitively coupled $\lambda/4$ short-circuited line and with identical capacitively coupled input and output lines. The input and output lines can be open ends with $\lambda/4$ length or short ends with $\lambda/2$ length, where λ is the wavelength at the center frequency. The filter circuit is configured on a two-layered structure to obtain capacitive coupling as shown in Fig. 1.

The filter design starts with analyzing the coupling structure of the $\lambda/4$ open T-resonator and capacitively coupled $\lambda/4$ short-circuited line as shown in Fig. 2. To obtain two transmission zeros as shown in Fig. 3, we introduce the capacitively coupled $\lambda/4$ short-circuited line below the shunt stub of the T-resonator. The $\lambda/4$ open stub functions like a series resonant circuit and the $\lambda/4$ short-circuited line like a parallel resonant circuit. These two resonant structures are capacitively coupled (C_0). The equivalent network of the two coupled circuits and its resultant transformation network are shown in Figs. 2(b) and 2(c). Two transmission zeros are introduced by the equivalent network as shown in Fig. 2[24].

$$Z_{in_s} = j\frac{(Z_{se}-Z_{so})^2-(Z_{se}+Z_{so})^2\cos^2\theta}{2(Z_{se}+Z_{so})\sin\theta\cos\theta} \tag{1}$$

$$[ABCD]_s = \begin{bmatrix} 1 & 0 \\ 1/Z_{in_s} & 1 \end{bmatrix} \tag{2}$$

$$S_{21} = \frac{2}{A+B/Z_0+CZ_0+D} = \frac{2}{2+Z_0/Z_{in_s}} \tag{3}$$

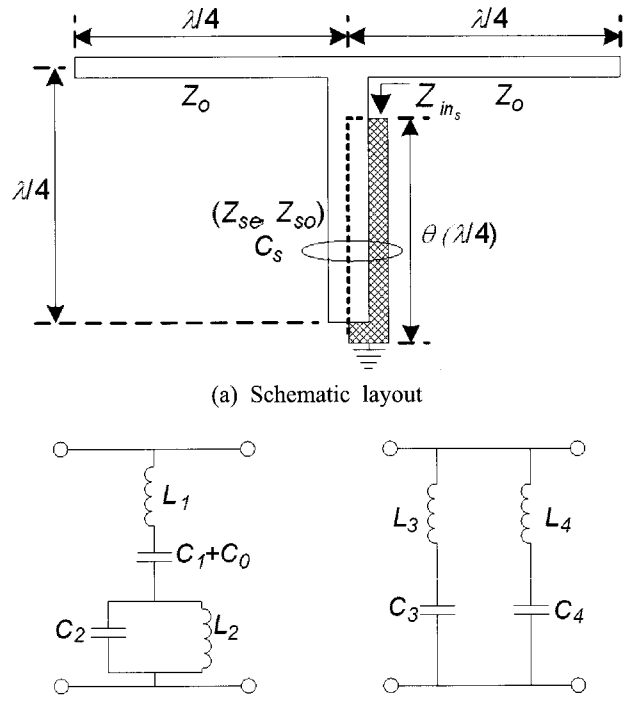

(a) Schematic layout

(b) Initial equivalent network (c) Resultant equivalent network

Fig. 2. Capacitively coupled $\lambda/4$ open T-resonator with $\lambda/4$ short-circuited line.

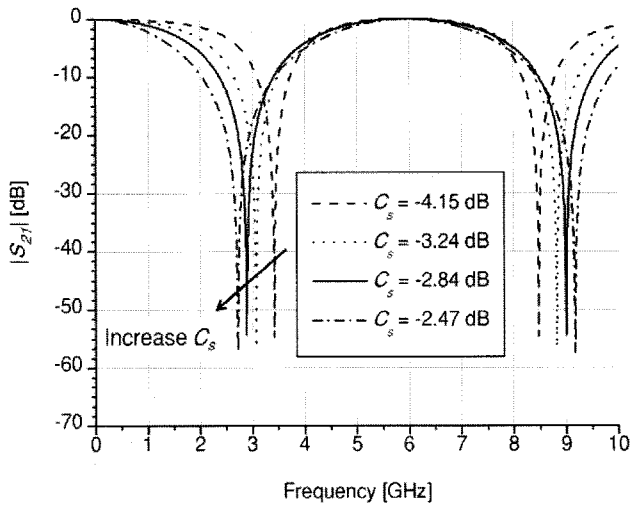

Fig. 3. Frequency response depending on capacitive coupling coefficient C_s between the T-resonator and the $\lambda/4$ short-circuited line.

$$S_{21} = \left\{ \left(Z_{se} - Z_{so}\right)^2 - \left(Z_{se} + Z_{so}\right)^2 \cos^2\theta \right\} / \{ \left(Z_{se} - Z_{so}\right)^2 - \left(Z_{se} + Z_{so}\right)^2 \cos^2\theta + -jZ_0 \left(Z_{se} + Z_{so}\right) \sin\theta \cos\theta \} \quad (4)$$

$$\cos\theta_z = \pm \frac{\left(Z_{se} - Z_{so}\right)}{\left(Z_{se} + Z_{so}\right)} = \pm C_s \quad (5)$$

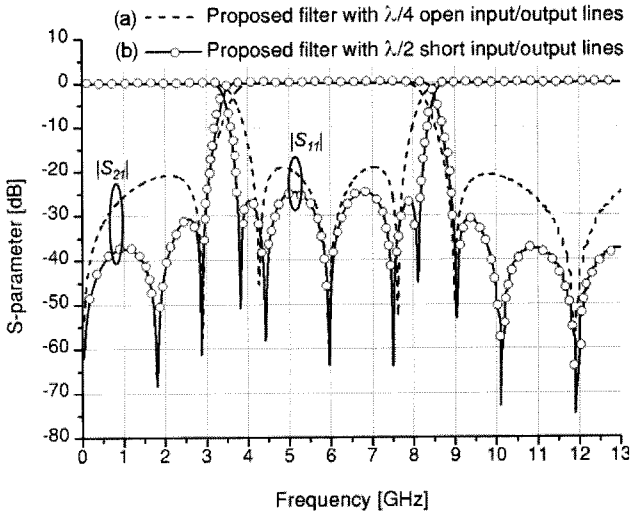

Fig. 4. Comparison of ADS simulation results for the two types of input/output lines with (a) $\lambda/4$ open ends or (b) $\lambda/2$ short ends.

$$f_z = f_o \frac{\theta_z}{\theta_o} \quad (6)$$

The input impedance(Z_{in_s}) of the coupled structure can be obtained from (1), where θ is the electrical length ($\lambda/4$) of the coupled structure, and Z_{se} and Z_{so} are even and odd characteristic impedances, respectively. The ABCD matrix for the coupled structure can be determined by (2) and the S_{21} is extracted with (3) and (4). Then, the relation between the coupling coefficient, C_s, of the coupled short-circuited line and positions of transmission zeros at lower and upper stop bands of the filter(θ_z or f_z) can be obtained by (5) and (6) in which f_o is the center frequency and $\theta_o = \pi/2$. The higher the value of the coupling coefficient C_s, the wider the bandwidth that can be realized between two transmission zeros as shown in Fig. 3.

By choosing the coupling coefficient C_s of -2.84 dB, two transmission zeros have been placed at 2.9 and 9.0 GHz near the pass band for the European band as shown in Fig. 4, respectively. The $\lambda/4$ input and output-coupled lines with the two main lines of the T-resonator add transmission zeros at DC and $2f_o$ regardless of the characteristic impedances of the coupled lines. Therefore, they are used to suppress the unwanted signals in the lower and upper stopbands. In this design, if the center frequency is located at f_o=5.95 GHz, two additional transmission zeros are placed at DC and 11.9 GHz by using the two input and output-coupled lines. To obtain rejection bands better than 20 dB, the impedances of even and odd modes of the coupled lines are set at 90.3

Ω and 22.96 Ω, respectively. Then, the 50 Ω input and output transmission lines are connected to the coupled lines as shown in Fig. 1.

$$[ABCD]_i = \begin{bmatrix} \frac{Z_{ie}+Z_{io}}{Z_{ie}-Z_{io}}\cos\theta & j\frac{(Z_{ie}-Z_{io})^2-(Z_{ie}+Z_{io})^2\cos^2\theta}{2(Z_{ie}-Z_{io})\sin\theta} \\ j\frac{2\sin\theta}{Z_{ie}-Z_{io}} & \frac{Z_{ie}+Z_{io}}{Z_{ie}-Z_{io}}\cos\theta \end{bmatrix} \quad (7)$$

$$[ABCD]_T = [ABCD]_i \times [ABCD]_s \times [ABCD]_i \quad (8)$$

$$S_{11} = \frac{A_T + B_T/Z_0 - C_T Z_0 - D_T}{A_T + B_T/Z_0 + C_T Z_0 + D_T}$$

$$S_{21} = \frac{2}{A_T + B_T/Z_0 + C_T Z_0 + D_T} \quad (9)$$

The $[ABCD]_i$ matrix of the coupled lines at the input or output can be written as (7) where Z_{ie} and Z_{io} are even and odd characteristic impedances of the coupled lines. Correspondingly, the $[ABCD]_T$ matrix of the whole filter in (8) can be obtained by multiplication of the transmission matrix of the short-circuited coupled line $[ABCD]_s$ as (2) and those of the input/output-coupled lines as (7) in sequence. Finally, the scattering matrix for the whole filter structure can be obtained by (9).

Next, by replacing the two $\lambda/4$ open-circuited lines with two $\lambda/2$ short-circuited lines for input and output lines as shown in Figs. 1 and 5, we were able to obtain two additional transmission zeros in the lower and upper rejection bands of the filter as shown in Fig. 4, where the dotted line shows the S-parameters of the filter structure with the $\lambda/4$ open ends for the input/output lines and the empty circled line the S-parameters of the filter with the $\lambda/2$ short ends. These transmission zeros are obtained by the edge-coupling(C_{s1}) between two $\lambda/2$ short-circuited lines and the broadside coupling(C_i) between the $\lambda/2$ short-circuited lines and the two arms of the T-resonator where C_{s1} is the edge-coupling coefficient between two $\lambda/4$ sections of the input/output

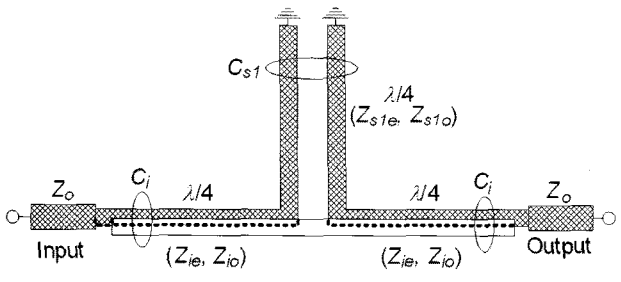

Fig. 5. Coupling structure for two additional transmission zeros in the rejection bands.

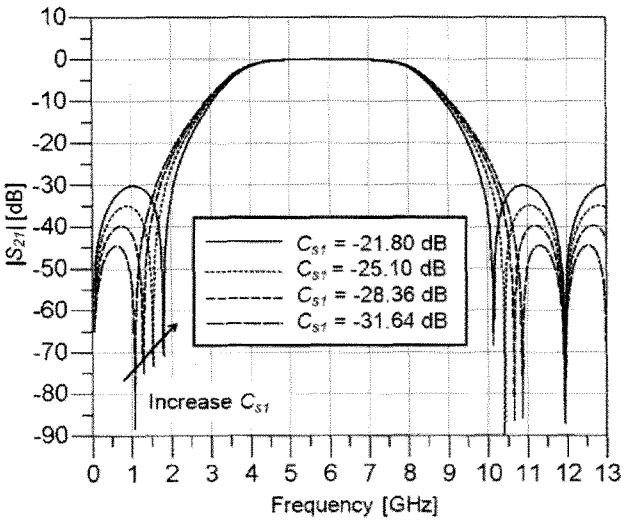

Fig. 6. Frequency response depending on the edge coupling coefficient C_{s1} between two $\lambda/4$ sections of the $\lambda/2$ short-circuited input/output lines.

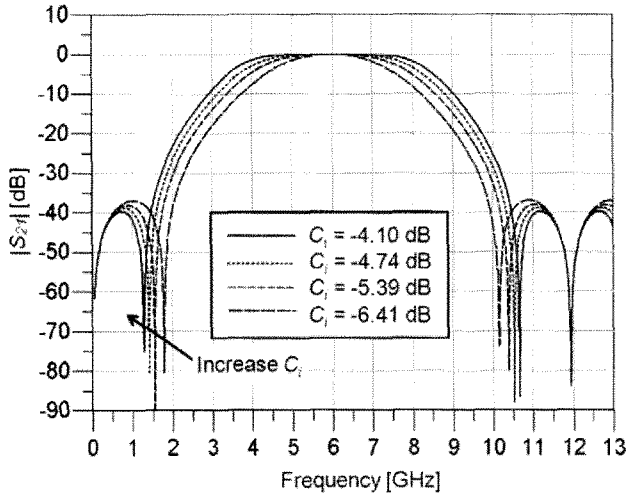

Fig. 7. Frequency response depending on the capacitive coupling coefficient C_i between the input/output lines and the T-resonator.

lines and C_i is the broadside coupling coefficient between the $\lambda/4$ sections of the input/output lines and the T-resonator as shown in Fig. 5. This structure provides a similar coupling between the short-circuited parallel-coupled line and the $\lambda/2$ slot-line resonator[25]. Figs. 6 and 7 show the effects on the bandwidth of the filter and on the locations of the two transmission zeros with respect to the coupling coefficients C_{s1} and C_i. The higher the value of C_{s1}, the narrower the bandwidth that can be obtained between two transmission zeros as shown in Fig. 6. In contrast with C_{s1}, the higher the value of C_i, the wider the bandwidth between two transmission zeros as shown in Fig. 7. In this study, C_{s1}

and C_i are set at -21.8 dB and -4.51 dB, respectively. Therefore, two additional transmission zeros have been added at 1.85 and 10.1 GHz.

ADS simulation results of the filter show flat and wide passband for European UWB applications and effectively suppressed unwanted passbands in the lower and upper stopband.

2-2 Equivalent Networks of the Bandpass Filter

The structure in Fig. 2(a) provides two transmission zeros and it can also be represented by two series of resonant circuits in parallel as discussed in Section 2-1. Therefore, the equivalent network for the proposed filter with $\lambda/4$-length open ends at the input/output line can be represented in terms of jX_{s1}, jX_{s2}, J and K inverters as shown in Fig. 8(a) and 8(b). This network is the same as that of the filter in [21]. The two K-inverters(K_1, K_2) represent the slope of two reactances, X_{s1} and X_{s2}, at around the center frequency and the two transmission zeros are differently formulated with the two K-inverters in Fig. 8(b)[20],[21]. The filter has three transmission poles within the pass band, one transmission pole comes from the $\lambda/4$ coupled short-circuited line below the T-resonator and the others come from input/output-coupled lines shown as the dotted lines in Fig. 4.

By using the $\lambda/2$-length short ends for the input/output lines, another two series of connected resonant networks can generate two additional transmission poles within the pass band. Therefore, the proposed filter has five transmission poles, which increase the selectivity of the filter. The edge-coupling between the two $\lambda/4$ sections of the $\lambda/2$-length short ends(upper part of Fig. 5) can be represented as a K-inverter connecting in parallel with the network in Fig. 8(b) as in [26]. Together with the two equivalent J-inverters formed by capacitively coupled input/output lines, the parallel K-inverter(K_3) enables two additional transmission zeros in the lower and upper stop bands of the filter which improve the stop band characteristics of the filter[20],[21].

2-3 Capacitively Coupled Double $\lambda/4$ Open T-Resonator

The filter developed for the European band shows very sharp characteristics at both lower and higher transitions bands. The bandwidth of the filter is proportional to the coupling of the input/output lines and that of the coupled $\lambda/4$ short-circuited line. In addition, the coupling depends mainly on the gap and width between the coupled lines. The maximum bandwidth of the filter structure in Fig. 1 under the conditions of the line width

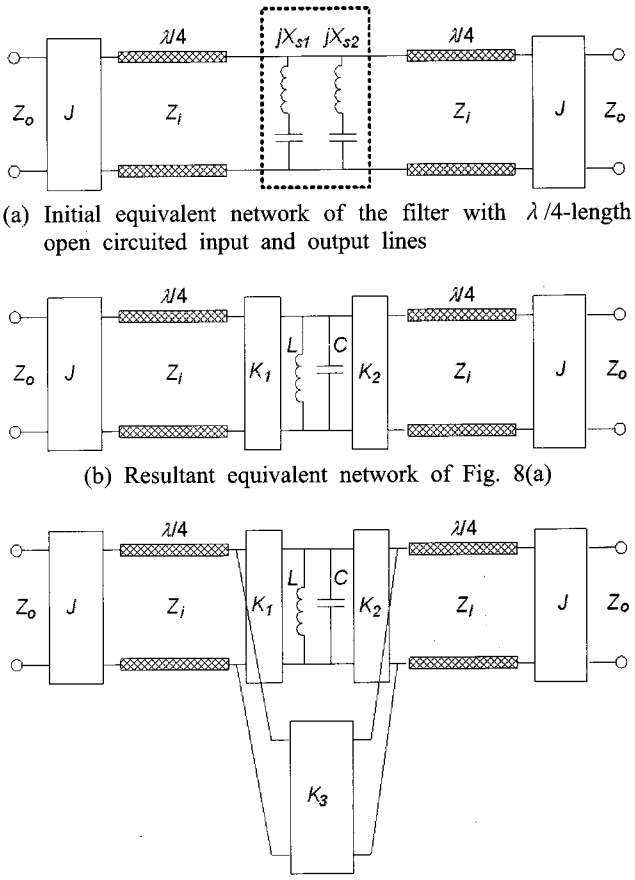

Fig. 8. Equivalent networks for the proposed filter.

of 70 μm and gap of 35 μm is about 6.0 GHz. For U.S. UWB applications with the frequency range from 3.1 to 10.6 GHz(7.5 GHz), we introduce two identical stacked $\lambda/4$ open T-resonators as shown in Fig. 9. The two $\lambda/2$ short circuited input/output lines and the $\lambda/4$ short circuited-line are placed between the two T-resonators.

By using this double capacitively coupled structure, both of the coupling coefficients C_s between the T resonator and the $\lambda/4$ short-circuited line and C_i between the T-resonator and the two $\lambda/4$ sections of the $\lambda/2$-length short input/output lines were increased. Therefore, the bandwidth of the filter was increased and the wider bandwidths between the first and second pair of transmission zeros were obtained as shown in Fig. 10, where the dotted line indicates the frequency response for the single T-resonator filter and the solid line shows that of the double T-resonator filter. Return loss better than 22 dB within the passband and insertion loss less than 33 dB out of band were achieved.

The bandwidth increment between the transmission zeros in the lower stopband(the ones near the pass band)

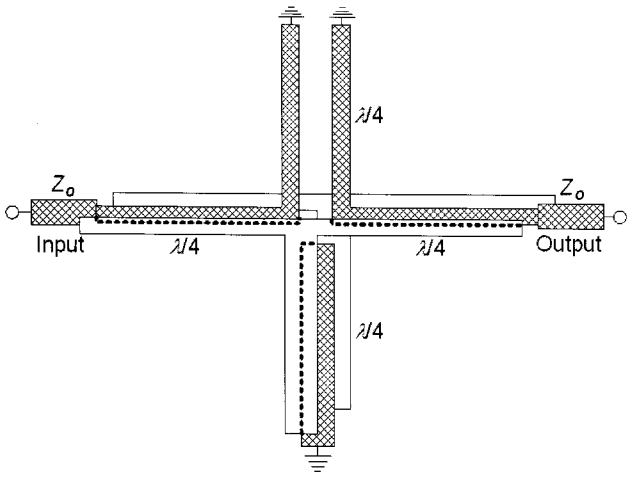

Fig. 9. Schematic for double T-resonator filter.

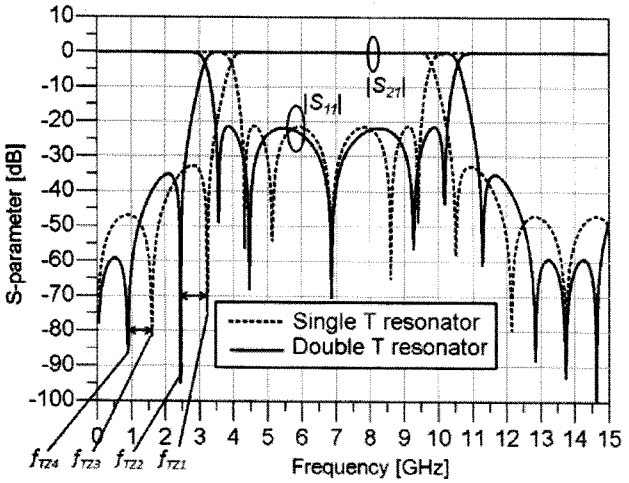

Fig. 10. Comparison of ADS simulation results for the single and double T-resonator UWB BPFs.

for the single T-resonator case(f_{TZ1}) and the double T resonator case(f_{TZ2}) with respect to the coupling coefficient C_s is about 0.69 GHz as shown in Fig. 11(a). Thus, we can calculate the locations of the transmission zeros for the double T-resonator from those of the single one. With the coupling coefficient C_s set at −2.768 dB, we were able to obtain two transmission zeros for the single T-resonator at 3.3 and 10.4 GHz. For the U.S. filter, two transmission zeros for the double T-resonator were placed at 2.61 and 11.09 GHz as shown in Fig. 10, Fig. 11(b) shows the bandwidth increment between the lowest transmission zeros for the single T-resonator case(f_{TZ3}) and the double T-resonator case(f_{TZ4}) with respect to the coupling coefficient C_i of the input/output-coupled lines. With C_i set at −3.71 dB, the related transmission zeros for the single T-resonator were placed at 1.55 and 12.15 GHz. And, the transmission zeros for the double T-resonator were observed at 0.94 and 12.76

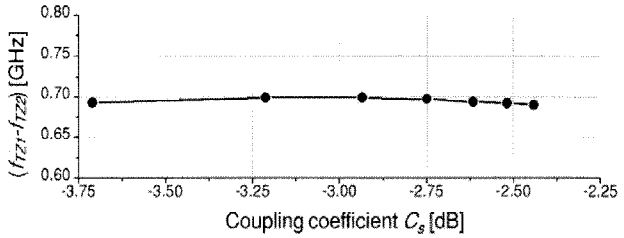

(a) $\lambda/4$ short-circuited line(C_s)

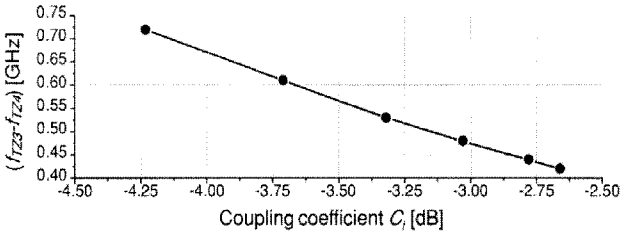

(b) Input/output lines(C_i)

Fig. 11. Bandwidth increments between the transmission zeros in the lower stopband for the single T-resonator(f_{TZ1}, f_{TZ3}) and for the double T-resonator(f_{TZ2}, f_{TZ4}) with respect to the coupling coefficient of the single T-resonator.

GHz, as shown in Fig. 10.

III. Field Simulation and Measurement Results

The filter structure with the single T-resonator as shown in Fig. 12 was simulated and tuned with the HFSS program. The structure consisted of 10 layers and each layer had a thickness of 50 μm and dielectric constant of 7.8. The filter patterns were located on the fifth and sixth layers. Via walls were added to the structure instead of solid walls in order to reduce the effects of interference. Due to the limitations of our LTCC manufacturing process, the distance between the two adjacent vias needed to be larger than 0.35 mm. This led to a slight deterioration of the performance of the filter. We measured the filter characteristics with the Anritsu ME7808A network analyzer and the Cascade Microtech Summit 12971B probe station and compared the measurement results with the simulation results. Fig. 13 shows the comparisons between the simulation and measurement results in terms of S-parameters and group delay for the filter with the single T resonator. The dotted line indicates the simulation results. The simulation results show a bandwidth of 5.3 GHz(3.3~8.6 GHz). The return loss is better than 16 dB, and insertion loss less than 0.3 dB in the passband. The group delay of the filter is about 0.25 ns at 5.95 GHz and has a variation within 0.2 ns from 3.8 GHz to 8.2 GHz. Attenuation slopes in the lower and upper transition bands are 102.7

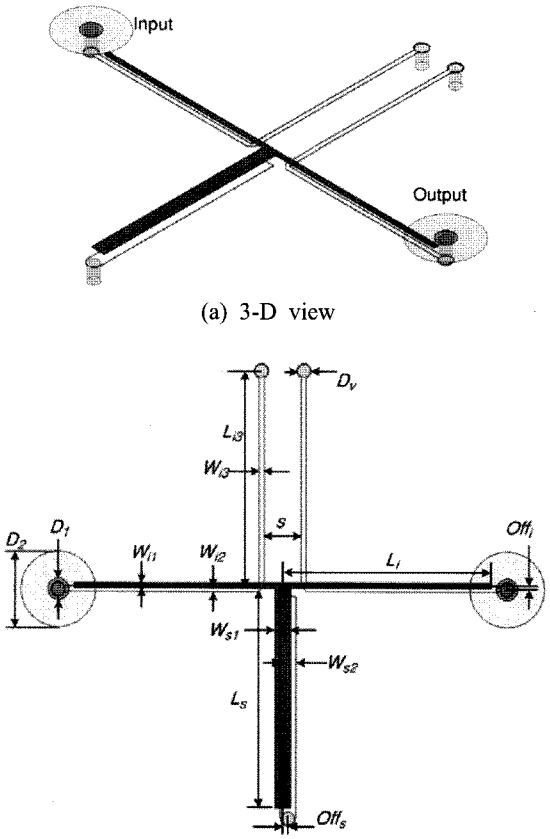

(a) 3-D view

(b) Top view

Fig. 12. The structure of the single T-resonator filter(W_{i1} =70 μm, W_{i2}=70 μm, W_{i3}=70 μm, W_{s1}=0.2 mm, W_{s2}=0.2 mm, L_i=4.375 mm, L_{i3}=4.27 mm, L_s= 4.265 mm, D_1= 0.2 mm, D_2= 0.7 mm, D_v= 0.12 mm, Off_i= 20 μm, Off_s= 20 μm, s= 0.42 mm).

dB/GHz and 97.3 dB/GHz, respectively. The filter has four transmission zeros at 1.85, 2.82, 9.0 and 10.85 GHz. Compared to the ADS simulation in Fig. 4, the transmission zeros in the upper rejection band have been shifted in the HFSS simulation. This is the effect of the T-junction making the length of two arms of T slightly larger than $\lambda/2$. The solid line shows the measurement results. A return loss better than 14 dB and insertion loss less than 0.9 dB were measured. The group delay is 0.26 ns at the center frequency and the group delay variation from 3.8 GHz to 8.2 GHz is less than 0.2 ns. The attenuation slope in the lower transition band is 96 dB/GHz. The attenuation slope in the upper transition band is 46 dB/GHz. The proposed filter has a compact size(10×10×0.5 mm^3) and has very sharp skirt characteristics with transmission zeros at lower and upper stopbands.

For U.S. UWB applications, the filter with double T-resonator as shown in Fig. 14 was simulated with the HFSS program and realized in LTCC technology. Green

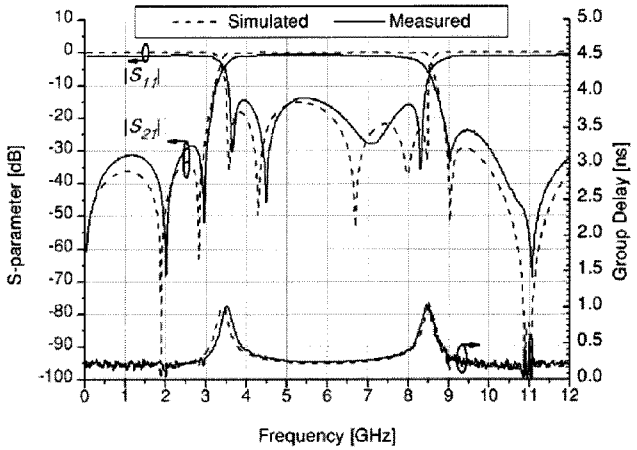

Fig. 13. Comparison of measured and simulated results for the filter shown in Fig. 12.

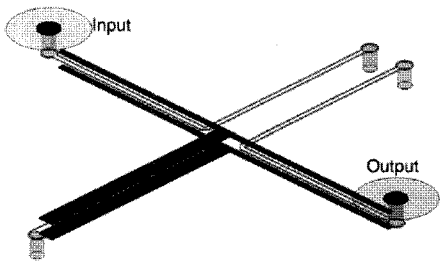

(a) 3-D view

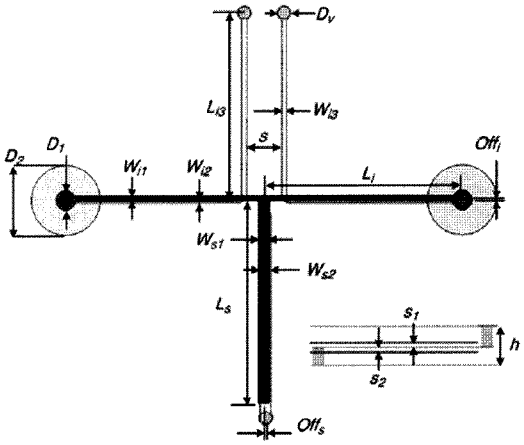

(b) Top view

Fig. 14. The structure of the double T-resonator filter(W_{i1} =70 μm, W_{i2}=70 μm, W_{i3}=70 μm, W_{s1}= 0.17 mm, W_{s2}=0.17 mm, L_i= 3.95 mm, L_{i3}=3.76 mm, L_s=3.81 mm, D_1=0.2 mm, D_2=0.7 mm, D_v= 0.12 mm, Off_i= 10 μm, Off_s= 15 μm, s_1= 35 μm, s_2= 35 μm, h= 315 μm, s= 0.38 mm).

tape with a thickness of 35 μm/layer and dielectric constant of 7.8 was used. The filter consisted of 10 layers and the two identical T-resonators were located on the fourth and sixth layers, and the input/output lines and

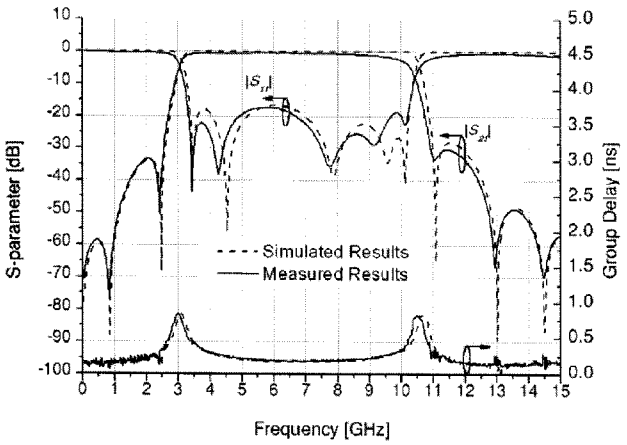

Fig. 15. Comparison of measured and simulated results for the filter shown in Fig. 14.

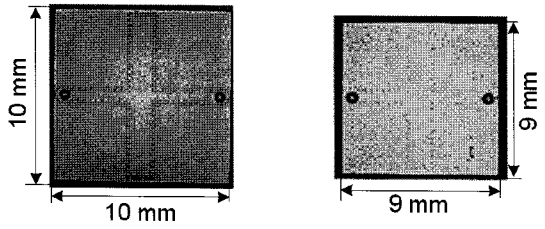

(a) Single T resonator (b) Double T-resonator

Fig. 16. Top view of the fabricated bandpass filters.

the $\lambda/4$ short-circuited line were on the fifth layer of the filter. Fig. 15 shows the comparison between the simulated and measured results for the filter in terms of S-parameters and group delay. The dotted line indicates the simulation results and the solid line the measurement results. The simulation results show a return loss better than 18 dB, and insertion loss less than 0.3 dB in the passband. The group delay of the filter is about 0.22± 0.25 ns for the frequency range from 3.5 GHz to 10.2 GHz. Attenuation slopes of both lower and upper skirts are steeper than 92 dB/GHz. The HFSS simulation shows that the filter has four transmission zeros at 0.85, 2.5, 11.1 and 12.9 GHz. A return loss better than 17 dB and insertion loss less than 0.8 dB were measured. The measured group delay varies between 0.22 ns and 0.4 ns for the frequency range from 3.5 GHz to 10.2 GHz. Attenuation slopes in the lower and higher transition bands are 67 dB/GHz and 39 dB/GHz, respectively. The size of the filter is 9×9×0.32 mm^3. Fig. 16 shows the top views of the two fabricated bandpass filters with the single T-resonator and the double T-resonator structures.

Ⅳ. Conclusion

In this paper, UWB band pass filters with elliptic function-type characteristics for the European and the U.S. bands were introduced in LTCC technology. We showed that the structure of the $\lambda/4$ open T-resonator and capacitively coupled $\lambda/4$ short line provides ultra-wideband characteristics. By using capacitively coupled $\lambda/2$ short input/output lines instead of $\lambda/4$ open input/output lines, sharper roll-off characteristics and two additional transmission zeros were realized in the lower and higher transmission bands of the filter. We also showed that the locations of the transmission zeros of the filters were determined based on the capacitive coupling of the T-resonators and the $\lambda/4$ short-circuited line and the inductive coupling of the two $\lambda/4$ sections of the two $\lambda/2$-length short-end input/ output lines. By using the double T-resonator, we found that bandwidth of the filter can be increased. The filters have compact size and measurement results agree well with simulation results. We expect that the sharp roll-off characteristics and compact structure of the filter make it very suitable for UWB systems, particularly in mobile home network applications.

The authors wish to acknowledge the financial support of LG Innotek and the measurement assistance of the KETI(Korea Electronics Technology Institute).

References

[1] "Revision of Part 15 of the Commission's Rules Regarding Ultra-Wide band Transmission System", Federal Communications Commission, 2006 [Online]. Available: http://ftp.fcc.gov/oet/info/rules/part15.

[2] A. Saito, H. Harada, and A. Nishikata, "Development of bandpass filter for Ultra-Wide Band(UWB) communication systems", *Proc. IEEE Conf. Ultra-Wide band Syst. Technol.*, pp. 76-80, Nov. 2003.

[3] H. Ishida, K. Araki, "Design and analysis of UWB bandpass filter with ring filter", *IEEE MTT-S Int. Microwave Symp. Dig.*, pp. 1307-1310, Jun. 2004.

[4] C. L. Hsu, F. C. Hsu, and J. T. Kuo, "Microstrip bandpass filter for Ultra-Wideband(UWB) wireless communications", *IEEE MTT-S Int. Microwave Symp. Dig.*, pp. 679-682, Jun. 2005.

[5] L. Zhu, S. Sun, and W. Menzel, "Ultra-Wideband (UWB) bandpass filters using multiple mode resonator", *IEEE Microwave Wireless Compon. Lett.*, vol. 15, no. 11, pp. 796-798, Nov. 2005.

[6] H. Wang, L. Zhu, and W. Menzel, "Ultra-wideband bandpass filter with hybrid microstrip/CPW structure", *IEEE Microwave Wireless Compon. Lett.*, vol. 15, no. 12, pp. 844-846, Dec. 2005.

[7] J. Gao, L. Zhu, W. Menzel, and F. Bogelsack, "Short-circuited CPW multiple-mode resonator for Ultra-Wideband(UWB) bandpass filter", *IEEE Micro-*

wave Wireless Compon. Lett., vol. 16, no. 3, pp. 104-106, Mar. 2006.

[8] T. Kuo, S. Lin, and C. H. Chen, "Compact ultra-wideband bandpass filters using composite microstrip-coplanar-waveguide structure", *IEEE Trans. Microwave Theory Tech.*, vol. 54, no. 10, pp. 3772-3778, Dec. 2000.

[9] R. Li, L. Zhu, "Compact UWB bandpass filter using stub-loaded multiple-mode resonator", *IEEE Microwave Wireless Compon. Lett.*, vol. 17, no. 1, pp. 40-42, Jan. 2007.

[10] S. W. Wong, L. Zhu, "EBG-embedded multiple-mode resonator for UWB bandpass filter with improved upper-stopband performance", *IEEE Microwave Wireless Compon. Lett.*, vol. 17, no. 6, pp. 421-423, Jun. 2007.

[11] J. A. Ruiz-Cruz, Y. Zhang, K. A. Zaki, A. J. Piloto, and J. Tallo, "Ultra-wideband LTCC ridge waveguide filters", *IEEE Microwave Wireless Compon. Lett.*, vol. 17, no. 2, pp. 115-117, Feb. 2007.

[12] P. K. Singh, S. Basu, and Y. H. Wang, "Planar ultra-wideband bandpass filter using edge coupled microstrip lines and stepped impedance open stub", *IEEE Microwave Wireless Compon. Lett.*, vol. 17, no. 9, pp. 649-651, Sep. 2007.

[13] H. Uchida, N. Yoneda, and Y. Konishi, "An elliptic-function bandpass filter utilizing left-handed operations of an inter-digital coupled line", *IEICE Trans. Electron.*, vol. E91-C, no. 11, pp. 1771-1777, Nov. 2008.

[14] C. P. Chen, Z. Ma, H. Nihei, and T. Anada, "Novel compact ultra-wideband bandpass filter with steep skirt selectivity", *Proc. 38th European Micro. Conf.*, pp. 849-852, Oct. 2008.

[15] R. L. Peterson, R. F. Drayton, "A CPW T-resonator technique for electrical characterization of microwave substrates", *IEEE Microwave Wireless Compon. Lett.*, vol. 12, no. 3, pp. 90-92, Mar. 2002.

[16] B. Jokanovic, M. Rakic, "Broadband electrical characterization of microwave substrate using T-resonator technique", *Proc. 6th Int. Conf. on Tele. in Modern Satelite, Cable and Broadcasting Services*, TELSIKS 2003, vol. 1, pp. 348-351, Oct. 2003.

[17] K. P. Latti, M. Kettunen, J. P. Strom, and P. Silventoinen, "A review of microstrip T-resonator method in determination of dielectric properties of printed circuit board materials", *IEEE Trans. Instrum. Meas.*, vol. 56, pp. 62-66, Oct. 2007.

[18] Y. S. Hijazi, D. Hanna, D. Fairweather, Y. A. Vlasov, and G. L. Larkins, Jr., "Fabrication of a superconducting MEM shunt switch for RF applications", *IEEE Trans. Appl. Superconduct.*, vol. 13, no. 2, pp. 700-703, Jun. 2003.

[19] L. G. Lawrence, J. Burke, M. Brzhezinskaya, Y. Hijazi, J. Martinez, D. Fairweather, Y. A. Vlasov, and G. L. Larkins, Jr., "Multi-tapped microstrip "T" resonator using MEM switch for tuning", *IEEE Trans. Appl. Superconduct.*, vol. 15, no. 2, pp. 1036-1039, Jun. 2005.

[20] J. R. Lee, J. H. Cho, and S. W. Yun, "New compact bandpass filter using microstrip $\lambda/4$ resonator with open stub inverter", *IEEE Microwave and Guide Wave Lett.*, vol. 10, no. 12, pp. 526-528, Dec. 2000.

[21] L. Zhu, W. Menzel, "Compact microstrip bandpass filter with two transmission zeros using a stub-tapped half-wavelength line resonator", *IEEE Microwave Wireless Compon. Lett.*, vol. 13, no. 1, pp. 16-18, Jan. 2003.

[22] J. S. Kim, N. S. Kim, W. G. Moon, S. G. Byeon, and H. Shin, "A novel broadband suspended substrate stripline filter using resonators with T-shaped open-circuited stubs", *IEEE MTT-S Int. Microwave Symp. Dig.*, pp. 917-920, Jun. 2007.

[23] K. Ma, K. C. B. Liang, R. M. Jayasuriya, and K. S. Yeo, "A wideband and high rejection multimode bandpass filter using stub perturbation", *IEEE Microwave Wireless Compon. Lett.*, vol. 19, no. 1, pp. 24-26, Jan. 2009.

[24] I. S. Kim, "Microstrip posts and dielectric resonators showing a steep slope at lower and upper stopband for bandpass properties", *IEEE Microwave Wireless Compon. Lett.*, vol. 10, no. 9, pp. 365-367, Sep. 2000.

[25] H. Kuan, M. H. Weng, R. Y. Yang, and W. L. Chen, "Bandpass performance of the short circuited quarter wavelength parallel coupled line excited by the slot-line resonator", *IEEE Microwave and Optical Tech. Lett.*, vol. 51, no. 2, pp. 301-303, Feb. 2009.

[26] E. Hanna, P. Jarry, E. Kerherve, J. M. Pham, and D. L. H. Tong, "Synthesis and design of a suspended substrate capacitive gap-parallel coupled line bandpass filter with one transmission zero", *Proc. 10th Int. Conf. on Electronics, Circuits and Systems, ICECS 2003*, vol. 2, pp. 547-550, Dec. 2003.

Thai Hoa Duong

was born in HCM City, Vietnam in 1981. He received the B.S. degree in Electrical Engineering from Ho Chi Minh City Univeristy of Technology, Vietnam in 2004. From 2005, he joined Kyung Hee University, South Korea as a M.S. and Ph.D. combined program. His research interests include the design, analysis, synthesis and miniaturization of microwave planar ultra-wide band bandpass filters and power divider/combiners for wireless communication systems.

Ihn Seok Kim(M'82)

was born in Seoul, Korea, on August 4, 1947. He received his B.E. degree in Electrical Engineering from Kyung Hee University in 1974 and his M.Sc. and Ph.D. degrees in Electrical Engineering from the University of Ottawa, Canada, in 1983 and 1991, respectively. From 1973 to 1992, he had worked for Korean Broadcasting Systems as an RF engineer, at Com Dev as technical staff, General Instrument of Canada as a senior engineer, the Canadian Space Agency as a research scientist, and the Korean Mobile Telecommunications Corporation as a senior researcher. In 1992, he joined Kyung Hee University, where he has been working on the modeling of various microwave structures, their applications to filters, power divider/combiners, and microwave oscillators. He also works in the EMI/C field as a member of the Korean delegation for the CISPR B/F and TC 77C committees. From February 1999 to February 2000, he was on sabbatical at ETH(Zurich) and the Motorola EM Lab(Ft. Lauderdale). He served as a reviewer for IEEE MTT and MWCL from 1998 to 2007.